Structural Engineering and Mechanics, *Vol. 75, No. 2 (2020) 133-144*
DOI: https://doi.org/10.12989/sem.2020.75.2.133

Dual-phase-lag model on microstretch thermoelastic medium with diffusion under the influence of gravity and laser pulse

Mohamed I.A. Othman*[1], Elsayed M. Abd-Elaziz[2a] and Ibrahim E.A. Mohamed[1b]

[1]Department of Mathematics, Faculty of Science, Zagazig University, P.O. Box 44519, Zagazig, Egypt
[2]Ministry of Higher Education, Zagazig Higher Institute of Eng. & Tech., Zagazig, Egypt

(Received October 8, 2019, Revised February 6, 2020, Accepted February 10, 2020)

Abstract. This investigation is to study the effect of gravitational field and diffusion on a microstretch thermoelastic medium heating by a non-Gaussian laser beam. The problem was studied in the context of the dual-phase-lag model. The normal mode analysis is used to solve the problem to obtain the exact expressions for the non-dimensional displacement components, the micro-rotation, the stresses, and the temperature distribution. The effect of time parameter, heat flux parameter and gravity response of three theories of thermoelasticity i.e. dual-phase-lag model (DPL), Lord and Shulman theory (L-S) and coupled theory (CT) on these quantities have been depicted graphically for a particular model.

Keywords: gravity; microstretch; dual-phase-lag; diffusion; laser pulse

1. Introduction

The theory of thermoelasticity is a branch of applied mechanics, which deals with the mechanical and thermal influences on elastic bodies under the effect of mechanical disturbances and/or non-uniform temperature fields. It is, thus, an extension of the conventional theory of isothermal elasticity of processes, in which deformation and stresses are produced not only by mechanical forces alone but also by temperature variation as well. Biot (1956) formulated the equations of the theory of coupled theory of thermo-elasticity to eliminate the paradox inherent in the classical uncoupled theory. In the coupled theory the equation of motion is a hyperbolic partial differential equation while the energy equation still remains parabolic. Lord-Shulman's theory is the first generalization of the coupled theory. The basis of the model proposed by Lord and Shulman (1967) was to modify Fourier's law of the heat conduction equation by introducing a new physical concept called a relaxation time needed for acceleration of the heat flow. The heat equation of this theory of the wave type, it automatically ensures finite speeds of propagation of heat and elastic waves. The remaining governing equations for this theory, namely, the equations of motions and constitutive relations, remain the same as those for the coupled and uncoupled theories. Green and Lindsay (1972) introduced another theory of generalized thermoelasticity, known as temperature rate-dependent theory of thermo-elasticity, including the rate of temperature in constitutive equations. It is based on a form of the entropy inequality proposed by Green and Laws (1972). It does not violate the Fourier's law of heat conduction when the body under consideration has a center of symmetry. This theory contains two constants that act as relaxation times and modifies all the equations of the coupled theory, not only the heat equation.

Ozisik and Tzou (1994), and Tzou (1995a, b) developed a new model called the dual phase-lag model for the heat transport mechanism in which Fourier's law is replaced by an approximation to the modification of Fourier's law with two different time translations for the heat flux and the temperature gradient. The modification of Fourier's law with two different times to take into account the micro-structural effects that arise in high-rate heat transfer. In addition to its applications in the ultrafast pulse laser heating, temperature pulse propagation in liquid helium, nonhomogeneous lagging response in porous media, thermal lagging response in amorphous materials, the DPL heat conduction equation also arises in describing the effects of material defects and thermo-mechanical coupling due to ultrafast heating such as Tzou (1997), Al-Nimr and Al-Huniti (2000), Chen (2002), Lee and Tsai (2008), Abdallah (2009), Othman *et al*. (2015), Othman and Abd-Elaziz (2015, 2017), Samia and Othman (2016), Marin and Nicaise (2016), Marin and Craciun (2017), Abualnour *et al*. (2019), Belbachir *et al*. (2019), Zarga *et al*. (2019), Alimirzaei *et al*. (2019), Mahmoudi *et al*. (2019).

Diffusion can be defined as the random walk, of an ensemble of particles, from regions of great concentration to regions of lower concentration. There is now a great deal of interest in the study of this phenomenon, due to its many applications in geophysics and industrial applications. In integrated circuit fabrication, diffusion is used to introduce "dopants" in controlled amounts into the semiconductor substrate. In particular, diffusion is used to form the base and emitter in bipolar transistors, form integrated resistors,

*Corresponding author, Assistant Professor
E-mail: m_i_a_othman@yahoo.com
[a] Ph.D.
E-mail: sayed_nr@yahoo.com
[b] Ph.D.
E-mail: aboahmed_19721972@yahoo.com

http://www.techno-press.com/journals/sem&subpage=7
ISSN: 1225-4568 (Print), 1598-6217 (Online)

form the source/drain regions in MOS transistors and dope poly-silicon gates in MOS transistors. Thermal diffusion utilizes the transfer of heat across a thin liquid or gas to accomplish isotope separation. Today, thermal diffusion remains a practical process to separate isotopes of noble gases (e.g. xexon) and other light isotopes (e.g. carbon) for research purposes. In most of the applications, the concentration is calculated using what is known as Fick's law. This is a simple law which does not take into consideration the mutual interaction between the introduced substance and the medium into which it is introduced or the effect of temperature on this interaction. However, there is a certain degree of coupling with temperature and temperature gradients as temperature speeds up the diffusion process. The diffusion in thermoelastic solids is due to the coupling of fields of temperature, mass diffusion and that of strain in addition to heat and mass exchange with the environment.

Nowacki (1974, 1976) developed the theory of coupled thermoelastic diffusion. This implies infinite speeds of propagation of thermoelastic waves. Problems of wave propagation in coupled or generalized diffusion thermo-elasticity have been studied by various researchers (Gawinecki *et al.* 2000, Gawinecki and Szymaniec 2002, Sharma and Kumar (2016), Singh 2005, Sharma *et al.* 2008, Othman and Marin 2017, Marin *et al.* 2019).

This paper investigates the effect of diffusion and laser pulse on a linear, isotropic, homogeneous microstretch thermoelastic solid influenced by the gravitational field based on DPL theory. The analytic methodology used to get the exact solutions of the considered physical quantities was the normal mode analysis. The variations of the considered variables are obtained and illustrated graphically. The effects of time, gravity, and heat flux parameter on the distributions of the considered variables are of concern and discussed in detail.

2. Basic equations

Following Eringen (1999) and Tzou (1995a) the equations of motion and the constitutive relations in a homogeneous isotropic microstretch thermoelastic diffusion solid in the absence of body forces, and in the presence of the body couples, the stretch force, and the heat sources, under the effect of Laser pulse Q with dual-phase-lag are given by,

$$(\lambda+2\mu+k)\underline{\nabla}(\underline{\nabla}.\underline{u})-(\mu+k)\underline{\nabla}\times(\underline{\nabla}\times\underline{u})+k\,\underline{\nabla}\times\underline{\phi} + \lambda_0\underline{\nabla}\phi^* - \beta_1\underline{\nabla}T - \beta_2\underline{\nabla}C = \rho\frac{\partial^2\underline{u}}{\partial t^2}, \tag{1}$$

$$(\alpha+\beta+\gamma)\underline{\nabla}(\underline{\nabla}.\underline{\phi})-\gamma\underline{\nabla}\times(\underline{\nabla}\times\underline{\phi})+k\,(\underline{\nabla}\times\underline{u})-2k\,\underline{\phi}=\rho j\frac{\partial^2\underline{\phi}}{\partial t^2}, \tag{2}$$

$$\alpha_0\nabla^2\phi^* + \frac{1}{3}\nu_1 T + \frac{1}{3}\nu_2 C - \frac{1}{3}\lambda_1\phi^* - \frac{1}{3}\lambda_0\underline{\nabla}.\underline{u} = \frac{3}{2}\rho j_0\frac{\partial^2\phi^*}{\partial t^2}, \tag{3}$$

$$k^*(1+\tau_\theta\frac{\partial}{\partial t})\nabla^2 T = (1+\tau_q\frac{\partial}{\partial t})(\beta_1 T_0\underline{\nabla}.\frac{\partial\underline{u}}{\partial t} + \nu_1 T_0\frac{\partial\phi^*}{\partial t} + \rho C_E\frac{\partial T}{\partial t} + aT_0\frac{\partial C}{\partial t} - \rho Q), \tag{4}$$

$$d\,\beta_2\nabla^2(\underline{\nabla}\underline{u}) + d\,\nu_2\nabla^2\phi^* + da\nabla^2 T + \frac{\partial C}{\partial t} - db\nabla^2 C = 0. \tag{5}$$

The constitutive relations are

$$\sigma_{ij} = (\lambda u_{r,r} + \lambda_1\phi^* - \beta_1 T - \beta_2 C)\delta_{ij} + \mu(u_{i,j} + u_{j,i}) + k\,(u_{j,i} - \varepsilon_{ijr}\phi_r), \tag{6}$$

$$m_{ij} = \alpha\phi_{r,r}\delta_{ij} + \beta\phi_{i,j} + \gamma\phi_{j,i} + b_0\varepsilon_{rji}\phi^*_{,r}, \tag{7}$$

$$\lambda^*_i = \alpha_0\phi^*_{,i} + b_0\varepsilon_{ijr}\phi_{j,r}. \tag{8}$$

where $\lambda, \mu, \alpha, \beta, \gamma, \alpha_0, b_0, \lambda_0, \lambda_1, k$ are material constants ρ is the mass density $\boldsymbol{u}$ is the displacement vector and ϕ is the micro rotation vector, ϕ^* is the scalar micro stretch function, T is the small temperature increment, T_0 the reference temperature of the body chosen such that $|(T-T_0)/T_0| \ll 1$, C is the concentration of the diffusion material in the elastic body, k^* is the coefficient of the thermal conductivity, C_E the specific heat at constant strain, a, b are the coefficients describing the measure of thermo diffusion and mass diffusion effects respectively, $\beta_1 = (3\lambda + 2\mu + k)\alpha_{t_1}$, $\beta_2 = (3\lambda + 2\mu + k)\alpha_{c_1}$, $\nu_1 = (3\lambda + 2\mu + k)\alpha_{t_2}$, $\nu_2 = (3\lambda + 2\mu + k)\alpha_{c_2}$, $\alpha_{t_1}, \alpha_{t_2}$ are the coefficients of linear thermal expansion and $\alpha_{c_1,}\alpha_{c_2}$ are the coefficients of linear diffusion expansion, d is the thermoelastic diffusion constant, j is the coefficients of micro-inertia, j_0 is the micro-inertia for the micro-elements, σ_{ij}, m_{ij}, are the components of stress and couple stress tensors respectively, δ_{ij} is the Kronecker delta, τ_θ is the phase-lag of the gradient of temperature, τ_q is the phase-lag of heat flux where $0 \le \tau_\theta \le \tau_q$.

The plate surface is illuminated by a laser pulse given by the heat input (Al-Qahtani and Datta 2008)

$$Q = \frac{I_0\gamma^*}{2\pi r^2 t_0^2}t\exp(\frac{-x^2}{r^2} - \frac{t}{t_0})\exp(-\gamma^* z). \tag{9}$$

Here t_0 $(t_0 = 0.01\,ps)$ is the pulse rise time, I_0 is the energy absorbed, r is the beam radius, and γ^* is the absorption coefficient.

3. Formulation and solution of the problem

We consider a homogeneous, isotropic generalized diffusion thermoelastic medium in the undeformed state at temperature T_0 The rectangular Cartesian coordinate system (x,y,z) having origin on the surface y=0 with the $y-$ axis pointing normally into the medium is introduced. For two dimensional problem, we assume the dynamic displacement vector as $\boldsymbol{u}(x,z,t)=(u,0,w)$, the micro rotation vector $\boldsymbol{\phi}$ = (0, ϕ_2, 0) the scalar micro stretch function $\phi^*(x,z,t)$ and we define the dimensionless, quantities as

$$\bar{x}_i=\frac{\omega^*}{C_1}x_i,\ \bar{u}_i=\frac{\rho C_1\omega^*}{\beta_1 T_0}u_i,\ \bar{T}=\frac{T}{T_0},$$
$$(\bar{\phi}^*,\bar{\phi}_2)=\frac{\rho C_1^2}{\beta_1 T_0}(\phi^*,\phi_2),$$
$$(\bar{t},\bar{\tau}_\theta,\bar{\tau}_q)=\omega^*(t,\tau_\theta,\tau_q),\ \bar{\sigma}_{ij}=\frac{\sigma_{ij}}{\beta_1 T_0},\ \bar{g}=\frac{g}{C_1\omega^*},\tag{10}$$
$$\bar{C}=\frac{\beta_2}{\rho^2 C_1^2}C,$$
$$(\bar{\lambda}_i^*,\bar{m}_{ij})=\frac{\omega^*}{C_1\beta_1 T_0}(\lambda_i^*,m_{ij}),\ \bar{Q}=\frac{\rho C_1^2}{k^* T_0\omega^{*2}}Q.$$

where $\omega^*=\dfrac{\rho C_E C_1^2}{k^*},\ C_1^2=\dfrac{\lambda+2\mu+k}{\rho}$ and ω^* is the characteristic frequency of the medium.

We introduce the potential functions $q(x,z,t)$, $\psi(x,z,t)$ such that

$$u=q_{,x}-\psi_{,z},\quad w=q_{,z}+\psi_{,x}.\tag{11}$$

From Eqs. (10) and (11) into the basic governing equations we obtain, (dropping the dashed for convenience),

$$(a_{20}\nabla^2-\frac{\partial^2}{\partial t^2})q+a_4\phi^*-T-a_5C-g\frac{\partial\psi}{\partial x}=0,\tag{12}$$

$$(a_2\nabla^2-\frac{\partial^2}{\partial t^2})\psi-a_3\phi_2+g\frac{\partial q}{\partial x}=0,\tag{13}$$

$$(a_6\nabla^2-2a_7-\frac{\partial^2}{\partial t^2})\phi_2+a_7\nabla^2\psi=0,\tag{14}$$

$$(a_8\nabla^2-a_{10}-\frac{\partial^2}{\partial t^2})\phi^*+a_{29}T+a_9C-a_{11}\nabla^2 q=0,\tag{15}$$

$$\begin{aligned}&[(1+\tau_\theta\frac{\partial}{\partial t})\nabla^2-a_{14}(\frac{\partial}{\partial t}+\tau_q\frac{\partial^2}{\partial t^2})]T-a_{12}(\frac{\partial}{\partial t}+\tau_q\frac{\partial^2}{\partial t^2})\nabla^2 q\\&-a_{13}(\frac{\partial}{\partial t}+\tau_q\frac{\partial^2}{\partial t^2})\phi^*-a_{15}(\frac{\partial}{\partial t}+\tau_q\frac{\partial^2}{\partial t^2})C=-(1+\tau_q\frac{\partial}{\partial t})Q,\end{aligned}\tag{16}$$

$$a_{16}\nabla^4 q+a_{17}\nabla^2\phi^*+a_{18}\nabla^2 T-(a_{19}\frac{\partial}{\partial t}+\nabla^2)C=0.\tag{17}$$

where the constants $a_i\ (i=1,2,....,30)$ are defined in the Appendix A.

The solution of the considered physical variable can be decomposed in terms of the normal modes in the following form

$$\{\phi^*,\phi_2,q,T,\psi,\sigma_{ij},m_{ij},C\}(x,z,t)=\{\bar{\phi}^*,\bar{\phi}_2,\bar{q},\bar{T},\bar{\psi},\bar{\sigma}_{ij},\bar{m}_{ij},\bar{C}\}(z)\,.\exp(\omega t+iRx).\tag{18}$$

where R is the wave number and ω is the frequency.

From (18) in (12)-(17) we obtained

$$(a_{20}\mathrm{D}^2-A_1)\bar{q}-A_2\bar{\psi}+a_4\bar{\phi}^*-\bar{T}-a_5\bar{C}=0,\tag{19}$$

$$(a_2\mathrm{D}^2-A_3)\bar{\psi}+A_2\bar{q}-a_3\bar{\phi}_2=0,\tag{20}$$

$$(a_6\mathrm{D}^2-A_4)\bar{\phi}_2+(a_7\mathrm{D}^2-A_5)\bar{\psi}=0,\tag{21}$$

$$(a_8\mathrm{D}^2-A_6)\bar{\phi}^*-(a_{11}\mathrm{D}^2-A_7)\bar{q}+a_{29}\bar{T}+a_9\bar{C}=0,\tag{22}$$

$$(a_{16}\mathrm{D}^4-A_0\mathrm{D}^2+A_8)\bar{q}+(a_{17}\mathrm{D}^2-A_9)\bar{\phi}^*+(a_{18}\mathrm{D}^2-A_{10})\bar{T}-(\mathrm{D}^2-A_{11})\bar{C}=0,\tag{23}$$

$$\{\phi^*,\phi_2,q,T,\psi,\sigma_{ij},m_{ij},C\}(x,z,t)=\{\bar{\phi}^*,\bar{\phi}_2,\bar{q},\bar{T},\bar{\psi},\bar{\sigma}_{ij},\bar{m}_{ij},\bar{C}\}(z)\,.\exp(\omega t+iRx).\tag{24}$$

Eliminating ψ, ϕ_2, ϕ^* and T among (19)-(24), we obtain the differential equation

$$\begin{aligned}&(\mathrm{D}^{12}-A\,\mathrm{D}^{10}+B\,\mathrm{D}^8-E\,\mathrm{D}^6+F\,\mathrm{D}^4-G\,\mathrm{D}^2+H)\\&\{\bar{C},\bar{q},\bar{\phi}^*,\bar{T},\bar{\psi},\bar{\phi}_2\}=-Q_0\{N_1,N_2,N_3,N_4,N_5,N_6\}f(x,t)\mathrm{e}^{-\gamma^* z},\end{aligned}\tag{25}$$

where $D=\frac{d}{dz}$, $f(x,t)$, $A_i(i=1,2,\ldots,50)$ and A,B,E,F,G,H,N_i $(i=1,\ldots6)$, Q_0, are defined in the Appendix B.

Equation (25) can be factored as

$$\begin{aligned}&(\mathrm{D}^2-k_1^2)(\mathrm{D}^2-k_2^2)(\mathrm{D}^2-k_3^2)(\mathrm{D}^2-k_4^2)(\mathrm{D}^2-k_5^2)(\mathrm{D}^2-k_6^2)\{C,q,\phi^*,T,\psi,\phi_2\}\\&=-Q_0\{N_1,N_2,N_3,N_4,N_5,N_6\}f(x,t)\mathrm{e}^{-\gamma^* z}.\end{aligned}\tag{26}$$

where $k_n^2(n=1,2,3,4,5,6)$ are the roots of the characteristic equation of the homogeneous equation of Eq. (25).

The general solution of (26) bounded as $z\to\infty$, is given by

$$q(x,z,t)=\sum_{n=1}^{6}M_n\exp(-k_n z+\omega t+iRx)+Q_0N_2L_1f(x,t)\mathrm{e}^{-\gamma^* z},\tag{27}$$

$$\psi(x,z,t)=\sum_{n=1}^{6}M_n\,\mathrm{H}_{2n}\exp(-k_n z+\omega t+iRx)+Q_0N_5L_1f(x,t)\mathrm{e}^{-\gamma^* z},\tag{28}$$

$$\phi_2(x,z,t)=\sum_{n=1}^{6}M_n\,\mathrm{H}_{1n}\exp(-k_n z+\omega t+iRx)+Q_0N_6L_1f(x,t)\mathrm{e}^{-\gamma^* z},\tag{29}$$

$$T(x,z,t)=\sum_{n=1}^{6}M_n\,\mathrm{H}_{4n}\exp(-k_n z+\omega t+iRx)+Q_0N_4L_1f(x,t)\mathrm{e}^{-\gamma^* z},\tag{30}$$

$$\phi^*(x,z,t)=\sum_{n=1}^{6}M_n\,\mathrm{H}_{3n}\exp(-k_n z+\omega t+iRx)+Q_0N_3L_1f(x,t)\mathrm{e}^{-\gamma^* z},\tag{31}$$

$$\mathrm{C}(x,z,t)=\sum_{n=1}^{6}M_n\,\mathrm{H}_{5n}\exp(-k_n z+\omega t+iRx)+Q_0N_1L_1f(x,t)\mathrm{e}^{-\gamma^* z}.\tag{32}$$

To obtain the components of the displacement vector, from (27) and (28) in (11)

$$u(x,z,t)=\sum_{n=1}^{6}M_nH_{7n}\exp(-k_nz+\omega t+iRx)+Q_0d_{38}f(x,t)\mathrm{e}^{-\gamma^* z}, \quad (33)$$

$$w(x,z,t)=\sum_{n=1}^{6}M_nH_{8n}\exp(-k_nz+\omega t+iRx)+Q_0d_{39}f(x,t)\mathrm{e}^{-\gamma^* z}, \quad (34)$$

$$e(x,z,t)=\sum_{n=1}^{6}M_nH_{6n}\exp(-k_nz+\omega t+iRx)+Q_0d_{37}f(x,t)\mathrm{e}^{-\gamma^* z}. \quad (35)$$

The stress tensor and the couple stress tensor and the microrotation from (6)-(8), dimensionless quantities are given by.

$$\sigma_{xx}(x,z,t)=\sum_{n=1}^{6}M_nH_{9n}\exp(-k_nz+\omega t+iRx)+Q_0d_{40}f(x,t)\mathrm{e}^{-\gamma^* z}, \quad (36)$$

$$\sigma_{yy}(x,z,t)=\sum_{n=1}^{6}M_nH_{10n}\exp(-k_nz+\omega t+iRx)+Q_0d_{41}f(x,t)\mathrm{e}^{-\gamma^* z}, \quad (37)$$

$$\sigma_{zz}(x,z,t)=\sum_{n=1}^{6}M_nH_{11n}\exp(-k_nz+\omega t+iRx)+Q_0d_{42}f(x,t)\mathrm{e}^{-\gamma^* z}, \quad (38)$$

$$\sigma_{xz}(x,z,t)=\sum_{n=1}^{6}M_nH_{12n}\exp(-k_nz+\omega t+iRx)+Q_0d_{43}f(x,t)\mathrm{e}^{-\gamma^* z}, \quad (39)$$

$$\sigma_{zx}(x,z,t)=\sum_{n=1}^{6}M_nH_{13n}\exp(-k_nz+\omega t+iRx)+Q_0d_{44}f(x,t)\mathrm{e}^{-\gamma^* z}, \quad (40)$$

$$m_{xy}(x,z,t)=\sum_{n=1}^{6}M_nH_{14n}\exp(-k_nz+\omega t+iRx)+Q_0d_{45}f(x,t)\mathrm{e}^{-\gamma^* z}, \quad (41)$$

$$m_{zy}(x,z,t)=\sum_{n=1}^{6}M_nH_{15n}\exp(-k_nz+\omega t+iRx)+Q_0d_{46}f(x,t)\mathrm{e}^{-\gamma^* z}, \quad (42)$$

$$\lambda_x^*(x,z,t)=\sum_{n=1}^{6}M_nH_{16n}\exp(-k_nz+\omega t+iRx)+Q_0d_{47}f(x,t)\mathrm{e}^{-\gamma^* z}, \quad (43)$$

$$\lambda_z^*(x,z,t)=\sum_{n=1}^{6}M_nH_{17n}\exp(-k_nz+\omega t+iRx)+Q_0d_{48}f(x,t)\mathrm{e}^{-\gamma^* z}. \quad (44)$$

where $H_{in},(i=1,\ldots,17),L_1$, and $d_i,(i=1,\ldots,48)$ are defined in the Appendix C.

4. Boundary conditions

In order to determine the parameters M_j, (j=1,2,3,4,5) we consider the boundary conditions at z=0, as follows:

$$\sigma_{zz}=\sigma_{zx}=m_{zy}=\lambda_z^*=\frac{\partial C}{\partial z}=0, \quad T=f_1e^{(\omega t+iRx)}. \quad (45)$$

where f_1 is constant, from (45) in (38), (40), (42), (44), (32), (30), and solving these equations for Mj, (j=1,2,3,4,5) by using the inverse of matrix method and the Matlab program we can obtain

$$\begin{pmatrix}M_1\\M_2\\M_3\\M_4\\M_5\\M_6\end{pmatrix}=\begin{pmatrix}H_{41}&H_{42}&H_{43}&H_{44}&H_{45}&H_{46}\\H_{51}k_1&H_{52}k_2&H_{53}k_3&H_{54}k_4&H_{55}k_5&H_{56}k_6\\H_{111}&H_{112}&H_{113}&H_{114}&H_{115}&H_{116}\\H_{131}&H_{132}&H_{133}&H_{134}&H_{135}&H_{136}\\H_{151}&H_{152}&H_{153}&H_{154}&H_{155}&H_{156}\\H_{171}&H_{172}&H_{173}&H_{174}&H_{175}&H_{176}\end{pmatrix}^{-1}\begin{pmatrix}f_1\\0\\0\\0\\0\\0\end{pmatrix}. \quad (46)$$

5. Special cases of microstretch thermoelastic theory:

(i) Equations of the microstretch thermoelastic with (DPL) theory when $\tau_\theta>\tau_q>0$.

(ii) Equations of the microstretch thermoelastic with the (L-S) theory when $\tau_\theta=0,\ \tau_q>0$.

(iii) Equations of the microstretch thermoelastic with (CT) theory when $\tau_\theta=0,\quad \tau_q=0$.

6. Numerical results and discussion

The analysis is conducted for a magnesium crystal-like material. Following Eringen (1984), the values of micro-polar parameters are,

$\lambda=9.4\times10^{10}Nm^{-2},\quad \mu=4.0\times10^{10}Nm^{-2},\quad k=1.0\times10^{10}Nm^{-2},$
$\rho=1.74\times10^3kgm^{-3},\ j=1.753\times10^{-15}m^{-2},\ j_0=0.2\times10^{-19}m^{-2},$
$\gamma=0.779\times10^{-9}N,\quad x=20.$

Thermal parameters are given by,

$C_E=1.04\times10^3jkg^{-1}k^{-1},\quad k^*=1.7\times10^6Jm^{-1}s^{-1}k^{-1},$
$\alpha_{t_1}=2.33\times10^{-5}k^{-1},\quad \alpha_{t_2}=2.48\times10^{-5}k^{-1},\quad f_1=1,$
$T_0=298k.$

Diffusion parameters are given by

$\alpha_{c_1}=2.65\times10^{-4}m^3kg^{-1}, \alpha_{c_2}=2.83\times10^{-4}m^3kg^{-1}, \tau^0=0.03,$
$b=32\times10^5kg^{-1}s^{-2}, d=0.85\times10^{-8}kgm^{-3}s, a=2.9\times10^4m^2s^{-2}k^{-1}.$

The laser pulse parameters are,

$I_0=10^5J/m^2,\ r=100\ \mu m,\ \gamma^*=10^{-3}m^{-1}.$

And, the microstretch parameters are taken as,

$\alpha_0=0.779\times10^{-9}N, \lambda_0=0.5\times10^{10}Nm^{-2}, \lambda_1=0.5\times10^{10}Nm^{-2}.$

The comparisons have established for two cases:

i) For two values of time (t=0.9 *sec*, 0.85 *sec*) in the context of DPL model, L-S theory and CT theory in the presence gravitational field (g=9.8) and laser pulse with the pulse duration (t_0=0.01 *p.sec*).

ii) For three values of heat flux parameter τ_q(τ_q=0.5, 0.55, 0.6) in the context of DPL theory in the presence gravitational field (g=9.8 and 9.5).

The numerical technique outlined above is used for the distribution of the real part of the non-dimensional displacement w, the non-dimensional temperature T, the distributions of the non-dimensional stress σ_{zz}, the non-dimensional micro-rotation ϕ_2, the concentration of the diffusion material in the elastic body C, the scalar micro-stretch function ϕ^*, and the micro-stress λ_x^* and the non-dimensional couple stress m_{zy} for the problem.

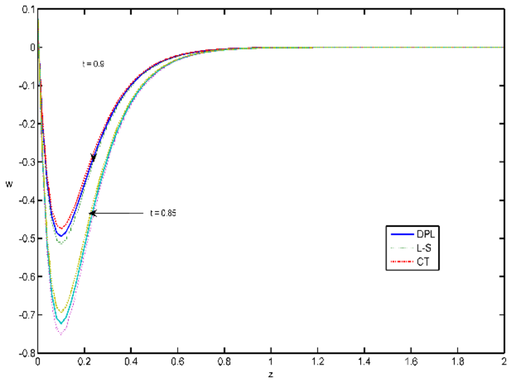

Fig. 1 Distribution of the displacement component w at two values of time

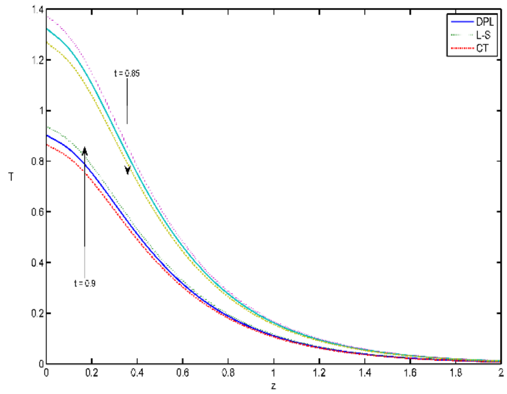

Fig. 2 Distribution of the temperature at two T values of time

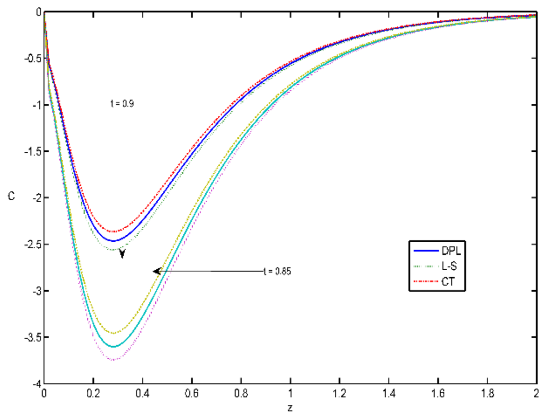

Fig. 3 Distribution of the concentration C at two values of time

The figures (1-8) are plotted to show the variation of the above quantities against the distance z in the context of (DPL) model, (L-S) theory and (CT) theory for two values of the time t=0.85, 0.9. Fig. 1 demonstrates that the distribution of the displacement w in the context of the three theories, begins from positive values and decreasing to negative values, then increasing to zero, it is also observed that the values of the displacement w at t=0.9 is greater than that at t=0.85 the value of w under the theory (CT) is greater

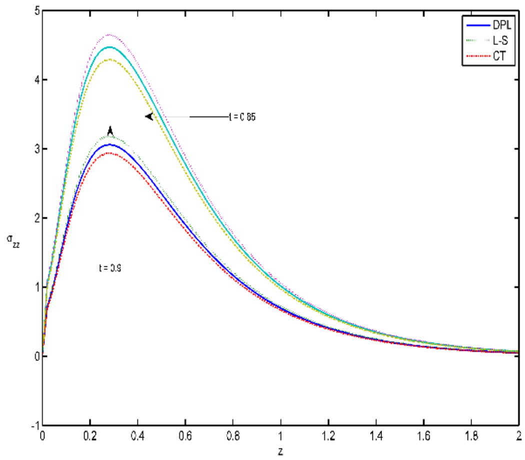

Fig. 4 Distribution of the stress component σ_{zz} at two values of time

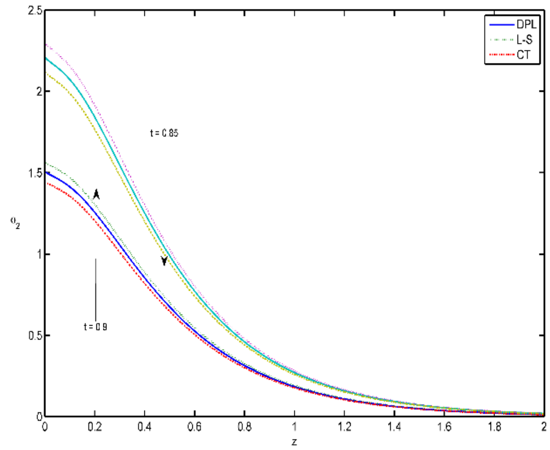

Fig. 5 Distribution the microrotation vector component ϕ_2 at two values of time

than that under the (DPL) model while it is smaller than that under the (L-S) theory. Fig. 2 depicts that the temperature T in the context of the three theories, begins from positive values and decreasing to zero, it is also noticed that the values of the temperature T at t=0.85, is greater than that at t=0.9, it is obvious that the temperature T under the theory (L-S) is greater than that under the (DPL) model while it is smaller than that under the (CT) theory. Fig. 3 depicts that the distribution of the diffusion C in the context of the three theories, begins from zero and decreasing to negative values then increasing to zero, It is also observed that the values of the diffusion C at t=0.9 is greater than that at t=0.85 it is obvious that the diffusion C under the theory (CT) is greater than that under the (DPL) model while it is smaller than that under the (L-S) theory. Fig. 4 shows that the stress σ_{zz} begins from zero and increasing to positive values, then decreasing to zero in the context of the three theories, it is also noticed that the values of the stress σ_{zz} at t=0.85 are greater than that at t=0.9, it is obvious that the stress σ_{zz} under the theory (L-S) is greater than that under the (DPL) model while it is smaller than that under the (CT) theory.

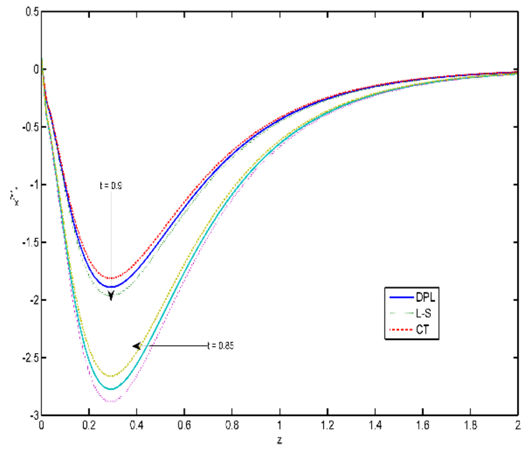

Fig. 6 Distribution of λ_x^* at two values of time

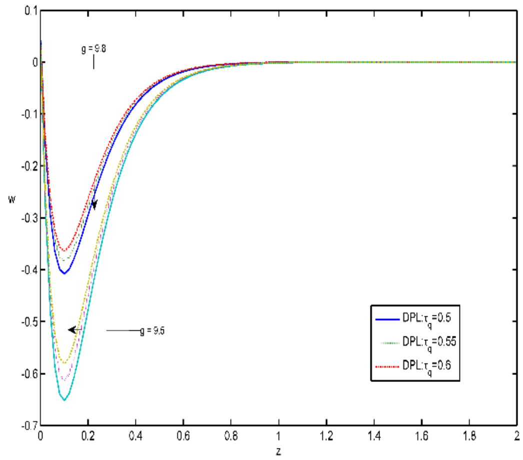

Fig. 9 Distribution of the displacement component w at two values of gravity

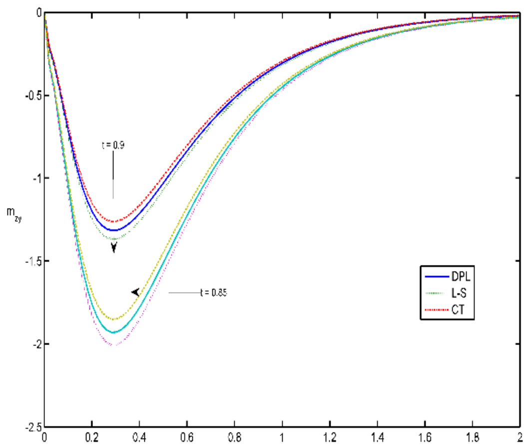

Fig. 7 Distribution of the couple stress m_{zy} at two values of time

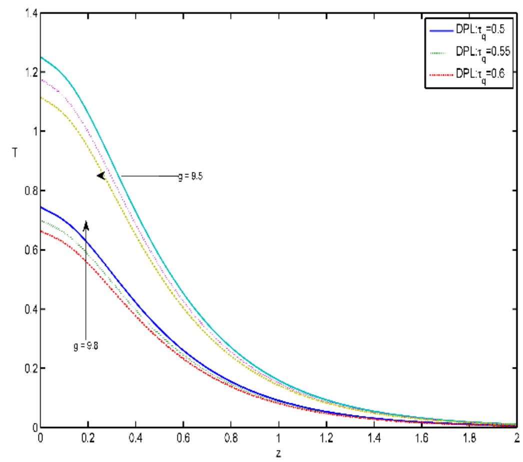

Fig. 10 Distribution of the temperature T at two values of gravity

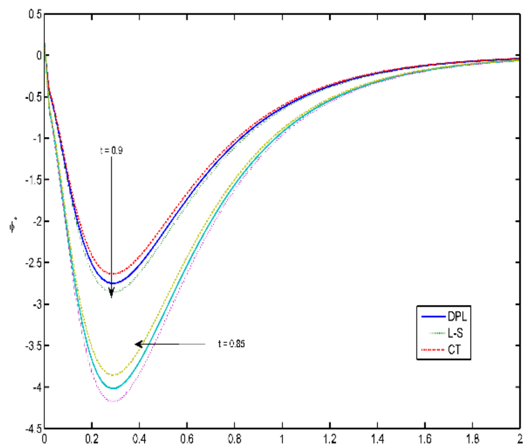

Fig. 8 Distribution of the scalar micro stretch function ϕ^* at two values of time

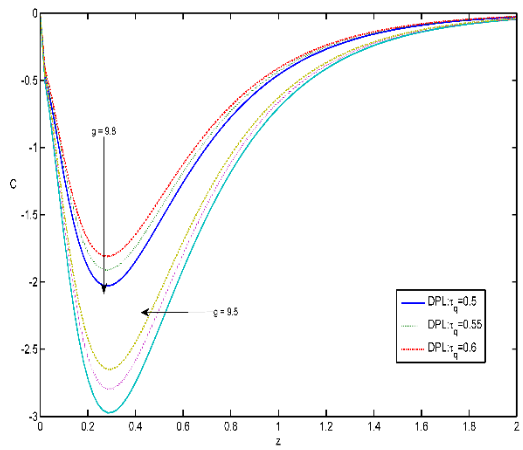

Fig. 11 Distribution of the concentration C at two values of gravity

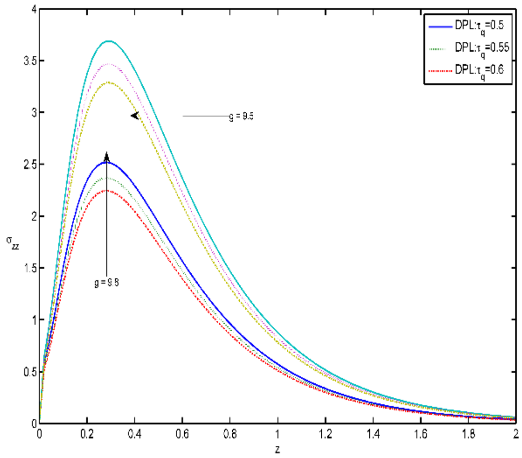

Fig. 12 Distribution of the stress component σ_{zz} at two values of gravity

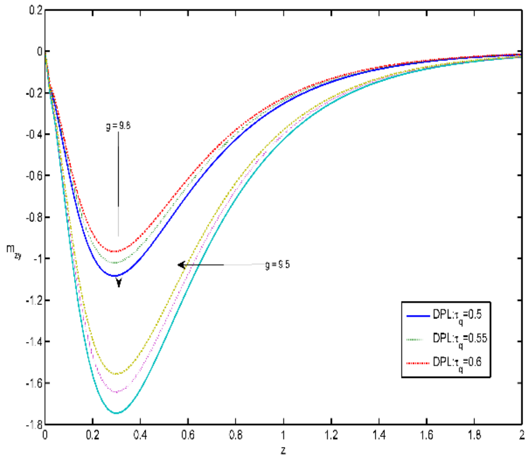

Fig. 15 Distribution of the couple stress m_{zy} at two values of gravity

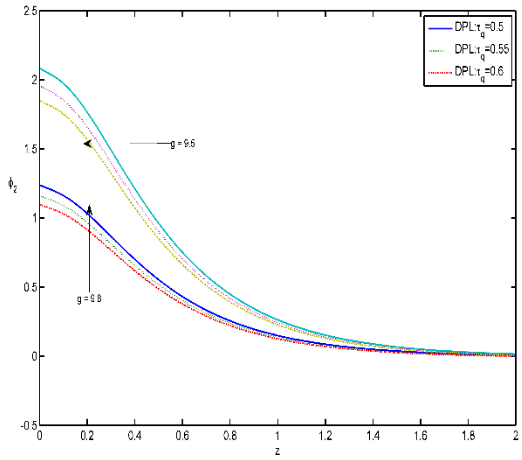

Fig. 13 Distribution of the microrotation vector component ϕ_2 at two values of gravity

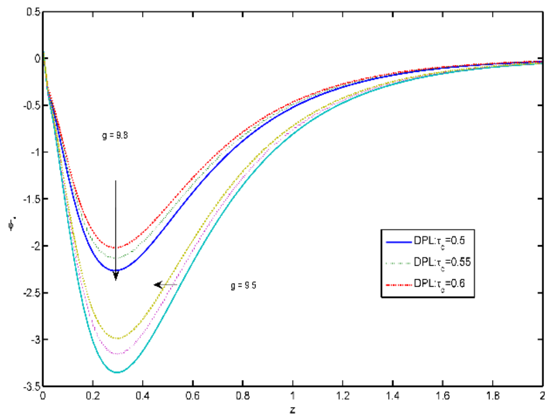

Fig. 16 Distribution of the scalar microstretch function ϕ^* at two values of gravity

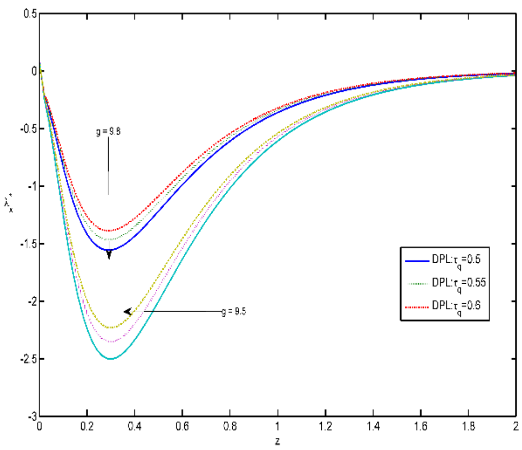

Fig. 14 Distribution of the micro-stress λ_x^* at two values of gravity

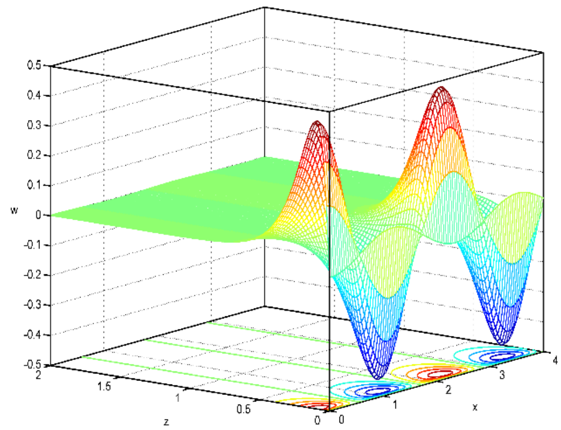

Fig. 17 3D Curve distribution of the displacement w versus the distances at: g=9.8, t = 0.9, I_0=10^5, τ_q =0.5, τ_θ =0.4

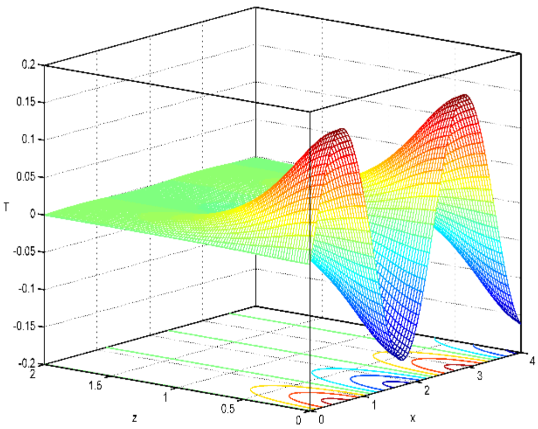

Fig. 18 3D Curve distribution of the temperature θ versus the distances at: g=9.8, t = 0.9, I_0=10^5, τ_q =0.5, τ_θ =0.4

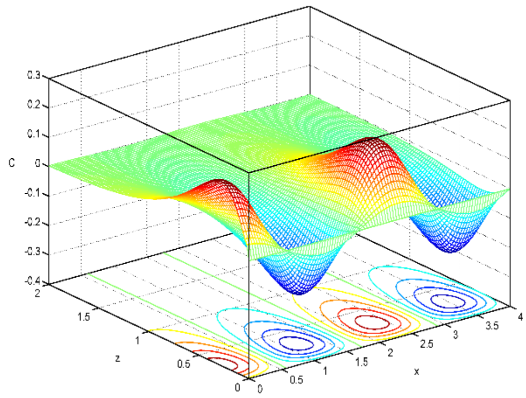

Fig. 19 3D Curve distribution of the concentration C versus the distances at: g=9.8, t = 0.9, I_0=10^5, τ_q =0.5, τ_θ =0.4

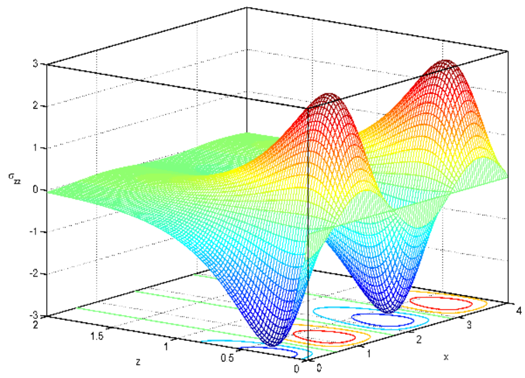

Fig. 20 3D Curve distribution of the stress component σ_{zz} versus the distances at: g=9.8, t = 0.9, I_0=10^5, τ_q =0.5, τ_θ =0.4

Fig. 5 demonstrates that the micro-rotation ϕ_2, begins from positive values and decreasing to zero in the context of the three theories, it is also noticed that the values of the micro-rotation ϕ_2 at t=0.85 are greater than that at t=0.9 and the micro-rotation ϕ_2 under the theory (L-S) is greater than that under the (DPL) model while it is smaller than that under the (CT) theory. Fig. 6 depicts that the distribution of λ_x^* in the context of the three theories, begins from positive values and decreasing to negative values, then increasing to zero, also, it is observed that the values of λ_x^*at t = 0.9 are greater than that at t = 0.85 It is clear that λ_x^* under the theory (CT) is greater than that under the (DPL) model, while it is smaller than that under the (L-S) theory. Fig. 7 shows that the couple stress m_{zy} begins from zero and decreasing to negative values, then increasing to zero in the context of the three theories, it is also noticed that the values of m_{zy} at t = 0.9 are greater than that at t = 0.85 and the couple stress m_{zy} under the theory (CT) is greater than that under the (DPL) model, while it is smaller than that under the (L-S) theory. Fig. 8 depicts that the distribution of the scalar microstretch function ϕ^* begins from positive values and decreasing to negative values, then increasing to zero, it is also noticed that the values of ϕ^* at t = 0.9 are greater than that at t = 0.85, it is obvious that the values of ϕ^*under the theory (CT) are greater than that under the (DPL) model while it is smaller than that under the (L-S) theory.

The figures (9-16) are plotted to show the variation of the above quantities against the distance z for three values of heat flux parameter τ_q(τ_q=0.5, 0.55, 0.6) in the context of (DPL) model in the presence gravitational field (g=9.8 and 9.5). Fig. 9 depicts that the distribution of the displacement w begins from positive values and decreasing to negative values then increasing to zero, it is also noticed that the values of the displacement w at g=9.8 are greater than that at g=9.8, it is obvious that the displacement w at τ_q=0.6 is greater than that at τ_q=0.55, while it is smaller than that at τ_q=0.5. Fig. 10 depicts that the temperature T in the context of the three theories, begins from positive values and decreasing to zero, it is also noticed that the values of the temperature T at g=9.8 are greater than that at g=9.8, it is obvious that the temperature T at τ_q=0.5is greater than that at τ_q=0.55 while it is smaller than that at τ_q=0.6. Fig. 11 depicts that the distribution of the diffusion C in the context of the three theories, begins from zero and decreasing to negative values, then increasing to zero, it is also observed that the values of the diffusion C at g=9.8 are greater than that at g=9.5, it is obvious that the diffusion C at τ_q=0.6 is greater than that at τ_q=0.55 while it is smaller than that at τ_q=0.5. Fig. 12 shows that the stress σ_{zz} begins from zero and increasing to positive values, then decreasing to zero in the context of the three theories, it is also noticed that the values of the stress σ_{zz} at g=9.5 are greater than that at g=9.8, it is obvious that the stress σ_{zz} at τ_q = 0.5 is greater than that at τ_q=0.55 while it is smaller than that at τ_q=0.6.

Fig. 13 demonstrates that the micro-rotation ϕ_2, begins from positive values and decreasing to zero in the context of the three theories, also, it is noticed that the values of the ϕ_2 at g=9.5 are greater than that at g=9.8 and the values of ϕ_2 at τ_q=0.5 are greater than that at τ_q=0.55 while it is smaller than that at τ_q=0.6. Fig. 14 depicts that the distribution of λ_x^* in the context of the three theories, begins from positive values and decreasing to negative values, then increasing to zero, it is also observed that the values of λ_x^* at g=9.8 are greater than that at g=9.5, it is obvious that the values of λ_x^* at τ_q=0.6 are greater than that at τ_q=0.55, while it is smaller than that at τ_q=0.5.

Fig. 15 shows that the couple stress m_{zy} begins from positive values and decreasing to negative values, then increasing to zero in the context of the three theories. It is also noticed that the values of the couple stress m_{zy} at g=9.8 are greater than that at g=9.5 and the couple stress m_{zy} at τ_q=0.6 is greater than that at τ_q=0.55 while it is smaller than at τ_q=0.5. Fig. 16 depicts that the distribution of the scalar microstretch function ϕ^* begins from positive values and decreasing to negative values, then increasing to zero. It is also noticed that the values of ϕ^* at g=9.8 are greater than that at g=9.5. It is clear that the values of ϕ^*at τ_q=0.6 are greater than that at τ_q=0.55, while it is smaller than that at τ_q=0.5.

Figures 17–20 are giving 3D surface curves for the physical quantities, i.e., the displacement w, the temperature T, the concentration of diffusion C, and the normal stress σ_{zz}, for the dual-phase-lag theory with diffusion by taking into account the effect of the gravity and laser pulse. The importance of these figures is that they give the dependence of the above physical sizes regarding the vertical component of distance.

7. Conclusion

According to the above results, we can conclude that: The value of all physical quantities converges to zero with an increase in distance z and all functions are continuous. The comparison of different theories of thermoelasticity, i.e. CT theory, L-S theory, and DPL theory are carried out. The analytical solutions based upon normal mode analysis for microstretch thermoelastic problems in solids have been developed and used. The deformation of a body depends on the nature of the applied forces and thermal loading due to laser pulse as well as the type of boundary conditions. The presence of gravity and laser pulse plays significant roles in all the physical quantities.

Declaration of conflicting interests

The author(s) declared no potential conflicts of interest withrespect to the research, authorship, and/or publication of this article.

Funding

The author(s) received no financial support for the research, authorship, and/or publication of this article.

References

Abdallah, I.A. (2009), “Dual phase lag heat conduction and thermoelastic properties of a semi-infinite medium induced by ultra-short pulsed laser”, *Progress Phys.,* **3**, 60-63.

Abualnour, M., Chikh, A., Hebali, H., Kaci, A., Tounsi, A., Bousahla, A.A. and Tounsi, A. (2019), “Thermomechanical analysis of anti-symmetric laminated reinforced composite plates using a new four variable trigonometric refined plate theory”, *Comput. Concr.*, **24**(6), 489-498. https://doi.org/10.12989/cac.2019.24.6.489

Alimirzaei, S., Mohammadimehr, M. and Tounsi, A. (2019), “Nonlinear analysis of viscoelastic micro-composite beam with geometrical imperfection using FEM: MSGT electro-magneto-elastic bending, buckling and vibration solutions”, *Struct. Eng. Mech*., **71**(5), 485-502. https://doi.org/ https://doi.org/10.12989/sem.2019.71.5.485

Al-Nimr, M.A. and Al-Huniti, N.S. (2000), “Transient thermal stresses in a thin elastic plate due to a rapid dual-phase-lag heating”, *J. Therm. Stress.*, **23**(8), 731–746. https://doi.org/10.1080/01495730050192383

Al-Qahtani, H.M. and Datta, S.K. (2008), “Laser-generalized thermoelastic waves in an anisotropic infinite plate: Exact analysis”, *J. Therm. Stress.*, **31**(6), 569-583. https://doi.org/10.1080/01495730801978380.

Biot, M.A. (1956), “Thermoelasticity and irreversible thermo-dynamics”, *J. Appl. Phys.*, **27**, 240-253. https://doi.org/10.1063/1.1722351.

Belbachir, N., Draich, K., Bousahla, A.A., Bourada, M., Tounsi, A. and Mohammadimehr, M. (2019), “Bending analysis of anti-symmetric cross-ply laminated plates under nonlinear thermal and mechanical loadings”, *Steel Compos. Struct.,* **33**(1), 81-92. https://doi.org/10.12989/scs.2019.33.1.081.

Chen, J.K., Beraun, J.E. and Tzou, D.Y. (2002), “Thermo-mechanical response of metals heated by ultra-short pulsed lasers”, *J. Therm. Stress.*, **25**(6), 539–558. https://doi.org/10.1080/01495730290074289.

Eringen, A.C. (1999), *Microcontinuum Field Theories I: Foundations and Solids*, Springer-Verlag, New York.

Eringen, A.C. (1984), “Plane wave in nonlocal micropolar elasticity”, *Int. J. Eng. Sci.*, **22**(8-10), 1113–1121. https://doi.org/10.1016/0020-7225(84)90112-5.

Gawinecki, J.A., Kacprzyk, P. and Bar-Yoseph, P. (2000), “Initial boundary value problem for some coupled nonlinear parabolic system of partial differential equations appearing in thermoelastic diffusion in solid body”, *J. Anal. Its Appl.*, **19**, 121-130.

Gawinecki, J.A. and Szymaniec, A. (2002), “Global solution of the Cauchy problem in nonlinear thermoelastic diffusion in solid body”, *Proc. Appl. Math. Mech.* (PAMM), **1**, 446-447.

Green, A.E. and Lindsay, K.A. (1972), “Thermoelasticity”, *J. Elast.*, **2**, 1-7. http://dx.doi.org/10.1007/BF00045689.

Green, A.E. and Laws, N. (1972), “On the entropy production inequality”, *Archive Rational Mechanics Analysis*, **45**(1), 47-53.

Lee, Y.M. and Tsai, T.W. (2008), “Effect of interfacial contact conductance on thermoelastic response in a two layered material heated by ultra-fast pulse-laser”, *J. Phys. D: Appl. Phys.*, **41**(4), 045308.

Lord, H.W. and Shulman, Y. (1967), “A generalized dynamical theory of thermoelasticity”, *J. the Mech. Phys. Solids*, **15**(4), 299-309. https://doi.org/10.1016/0022-5096 (67)90024-5.

Marin M., Othman, M.I.A., Vlase, S. and Codarcea-Munteanu, L., (2019), “Thermoelasticity of initially stressed bodies with voids. A domain of influence”, *Symmetry,* **11**(4), 573–584. doi:10.3390/sym1104057.

Marin, M., Baleanu, D. and Vlase. S. (2017), “Effect of microtemperatures for micropolar thermoelastic bodies”,Struct Eng*Mech*, **61**(3), 381-387. https://doi.org/ https://doi.org/10.12989/sem.2017.61.3.381.

Marin, M. and Craciun, E.M. (2017), “Uniqueness results for a boundary value problem in dipolar thermoelasticity to model composite materials”, *Compos. Part B Eng.,* **126**, 27-37. https://doi.org/10.1016/j.compositesb.2017.05.063.

Mahmoudi, A., Benyoucef, S. Tounsi, A., Benachour, A. Bedia, A.E. and Mahmoud, SR (2019), “A refined quasi-3D shear deformation theory for thermomechanical behavior of functionally graded sandwich plates on elastic foundations”, *J. Sandwich Struct. Mater.*, **21**(6), 1906-1926. https://doi.org/10.1177/1099636217727577.

Nowacki, W. (1974), “Dynamical problems of thermo-diffusion in solids I”, *Bull Acad Pol Sci Ser Sci Tech.*, **22**, 55-64.

Nowacki, W. (1976), “Dynamical problems of thermo-diffusion in solids”, *Eng. Fracture Mech.*, **8**, 261-266.

Othman, M.I.A., Hasona, W.M. and Mansour, N.T. (2015), “The influence of gravitational field on generalized thermoelasticity with two-temperature under three-phase-lag model”, *Comput. Mater. Continua*, **45**(3), 203-219.

Othman, M.I.A. and Abd-Elaziz, E.M. (2015), “The effect of thermal loading due to laser pulse on generalized thermoelastic medium with voids in dual phase lag model”, *J. Therm. Stress.*, **38**(9), 1068-1082. https://doi.org/10.1080/01495730290074289.

Othman, M.I.A. and Abd-Elaziz, E.M. (2017), “Effect of rotation and gravitational on a micropolar magneto-thermoelastic medium with dual-phase-lag model”, *Microsystem Technologies*, **23**, 4979–4987. https://doi.org/10.1007/s00542-017-3295-y.

Othman, M.I.A. and Marin, M. (2017), “Effect of thermal loading due to laser pulse on thermoelastic porous media under G-N theory”, *Results Phys.*, **7**, 3863-3872. https://doi.org/10.1016/j.rinp.2017.10.012.

Ozisik, M.N. and Tzou, D.Y. (1994), “On the wave theory of heat conduction”, *J. Heat Transfer* (ASME), **116**(3), 526-535. https://doi.org/10.1115/1.2910903.

Said, S.M. and Othman, M.I.A. (2016), “Wave propagation in a two-temperature fiber-reinforced magneto-thermoelastic medium with three-phase-lag model”, *Struct. Eng. Mech.*, **57**(2), 201-220. https://doi.org/10.1080/17455030.2019.1637552.

Sharma, N., Kumar, R. and Ram, P. (2008), “Plane strain deformation in generalized thermoelastic diffusion”, *Int. J. Thermophys.*, **29**(4), 1503-1522. https://doi.org/10.1007/s10765-008-0435-8

Sharma, V. and Kumar, S. (2016), “Influence of microstructure, heterogeneity and internal friction on SH waves propagation in a viscoelastic layer overlying a couple stress substrate“, *Struct Eng Mech*, **57**(4), 703-716. https://doi.org/10.12989/sem.2016.57.4.703

Singh, B. (2005), “Reflection of P and SV waves from free surface of an elastic soild with generalized thermodiffusion”, *J. Earth System Sci.*, **114**(2), 159- 168. https://doi.org/10.1007/BF02702017.

Tzou, D.Y. (1995a), “Experimental support for the lagging behavior in heat propagation”, *J. Thermophys. Heat Transfer*, 9(4), 686-693. https://doi.org/10.2514/3.725

Tzou, D.Y. (1995b), “A unified approach for heat conduction from macro to micro scales”, *J. Heat Transfer* (ASME) **117**(1), 8-16.
doi: https://doi.org/10.1115/1.2822329

Tzou, D.Y. (1997), *Macro-to Microscale Heat Transfer: The Lagging Behavior*, Taylor and Francis, New York, USA.

Zarga, D., Tounsi, A., Bousahla, A.A., Bourada, F. and Mahmoud, S.R. (2019), “Thermomechanical bending study for functionally graded sandwich plates using a simple quasi-3D shear deformation theory”, *Steel Compos. Struct.*, **32**(3), 389-410. https://doi.org/10.12989/scs.2019.32.3.389

CC

Appendix A

$$a_1=\frac{\mu+\lambda}{\rho c_1^2},\ a_2=\frac{k+\mu}{\rho c_1^2},\ a_3=\frac{k}{\rho c_1^2},\ a_4=\frac{\lambda_0}{\rho c_1^2},$$

$$a_5=\frac{\rho^2 c_1^2}{T_0\beta_1},\ a_6=\frac{2\Omega}{j\rho c_1^2},\ a_7=\frac{k}{\rho j\omega^{*2}},\ a_8=\frac{2\alpha_0}{3\rho j_0 c_1^2},$$

$$a_9=\frac{2\nu_2\rho^2 c_1^4}{9j_0\beta_1\beta_2 T_0\omega^{*2}},\quad a_{10}=\frac{2\lambda_1}{9\rho j_0\omega^{*2}},\quad a_{11}=\frac{2\lambda_0}{9\rho j_0\omega^{*2}},$$

$$a_{12}=\frac{\beta_1^2 T_0}{\rho k^*\omega^*},\quad a_{13}=\frac{\nu_1\beta_1 T_0}{\rho k^*\omega^*},\quad a_{14}=\frac{\rho C_E c_1^2}{k^*\omega^*},\quad a_{15}=\frac{a\rho^2 C_1^4}{k^*\beta_2\omega^*},$$

$$a_{16}=\frac{\beta_1\beta_2^2 T_0}{b\rho^2 c_1^2},\quad a_{17}=\frac{\beta_1\beta_2 T_0\nu_2}{b\rho^2 c_1^4},\quad a_{18}=\frac{a\beta_2 T_0}{b\rho c_1^2},\quad a_{19}=\frac{\rho c_1^2}{db\omega^*},$$

$$a_{20}=a_1+a_2,\quad a_{22}=\frac{\lambda_1}{\rho c_1^2},\ a_{23}=\frac{k+2\mu}{\rho c_1^2},\ a_{24}=\frac{\mu}{\rho c_1^2},$$

$$a_{25}=\frac{\gamma\omega^{*2}}{\rho c_1^4},\ a_{26}=\frac{b_0\omega^{*2}}{\rho c_1^4},\quad a_{27}=\frac{\beta\omega^{*2}}{\rho c_1^4},\quad a_{28}=\frac{\alpha_0\omega^{*2}}{\rho c_1^4},$$

$$a_{29}=\frac{2\nu_1 c_1^4}{9j_0\beta_1\omega^{*2}},\ a_{30}=\frac{\lambda}{\rho c_1^2},$$

Appendix B

$$f(x,t)=[\mathrm{n}_1 t-\mathrm{n}_0\tau_q(1-\frac{t}{t_0})]\exp(\frac{-x^2}{r^2}-\omega t-\mathrm{i}bx-\frac{t}{t_0}),$$

$$Q_0=\frac{\mathrm{I}_0\gamma^*}{2\pi r^2 t_0^2},\quad \delta_1=1+\tau_\theta\omega,\ \delta_2=1+\tau_q\omega,$$

$$s_1=a_9-a_5a_{29},\quad s_2=1+a_5a_{18},\ s_3=A_{10}+A_{11},$$

$$s_4=a_9-a_5a_{29},\ s_5=a_{17}+a_4a_{18},\ s_6=A_9+a_4A_{10},$$

$$s_7=A_6-a_4a_{29},\ s_8=a_8a_{20}-a_{11},\ s_9=a_8A_1-A_7,$$

$$s_{10}=a_{18}a_{20}s_1+a_{16}s_1+s_2s_8,$$

$$s_{11}=a_{18}A_1s_1+a_{20}s_1A_{10}+A_0s_1+s_3s_8+s_2s_9,$$

$$s_{12}=s_1A_1A_{10}+A_8s_1+s_3s_9,\ s_{13}=A_2(s_1a_{18}-a_8s_2),\ s_{14}=A_2(A_{10}s_1-s_3a_8),$$

$$s_{15}=s_4s_5-s_2s_7-s_3a_{29},\ s_{16}=s_4s_6-s_3s_7,\ A_1=a_{20}b^2+\omega^2,$$

$$A_2=ibg,\ A_3=a_2b^2+\omega^2,\ A_4=a_6b^2+2a_7+\omega^2.\ A_5=a_7b^2,$$

$$A_6=a_8b^2+a_{10}+\omega^2,\ A_7=a_{11}b^2,\ A_8=a_{16}b^4,\ A_9=a_{17}b^2,$$

$$A_{10}=a_{18}b^2,\ A_{11}=b^2-a_{19}\omega,\ A_{12}=\delta_1 b^2+a_{14}\delta_2,\ A_{13}=a_{12}\delta_2,$$

$$A_{14}=a_{12}\delta_2 b^2,\ A_{15}=a_{15}\delta_2,\ A_{16}=a_6A_3+a_2A_4-a_3a_7,\ A_{17}=A_3A_4-a_3A_5,$$

$$A_{18}=a_4A_{15}\text{-}a_5\delta_2a_{13},\ A_{19}=a_4a_{29}A_{15}+a_9\delta_2a_{13}-a_5a_{13}a_{29}\delta_2,$$

$$A_{20}=a_9-a_5a_{29},$$

$$A_{21}=a_{11}a_{18}A_{18}+a_{16}A_{19}+a_4a_{29}A_{13}+a_4a_9a_{18}A_{13}+a_{11}a_{17}A_{15}-a_{11}a_{13}\delta_2+a_{17}A_{13}A_{20},$$

$$A_{22}=a_{11}a_{10}A_{18}+a_{18}A_7A_{18}+A_0A_{19}+a_4a_{29}A_{14}+a_4a_{29}A_{11}A_{13}+a_4a_9A_{10}A_{13}+a_4a_9A_{14}A_{18}+a_{17}A_7A_{15}-a_{11}a_{13}A_{11}\delta_2-a_{13}A_7\delta_2+A_9A_{13}A_{20}+A_{14}A_{17}A_{20},$$

$$A_{23}=A_7A_{10}A_{18}+A_8A_{19}+a_4a_{29}A_{11}A_{14}+a_4a_9A_{10}A_{14}+A_7A_9A_{15}-a_{13}A_7A_{11}\delta_2+A_9A_{14}A_{20},$$

$$A_{24}=a_4a_9a_{16}\delta_1-a_4a_{11}\delta_1+a_8a_{16}A_{15}+a_8A_{13}+a_5a_{11}a_{17}\delta_1+a_5a_8a_{18}A_{13},$$

$$A_{25}=a_4a_9\delta_1A_0+a_4a_9a_{16}A_{12}-a_4a_{11}A_{12}-a_4a_{11}A_{11}\delta_1-a_4A_7\delta_1+a_8A_0A_{15}+a_{16}A_6A_{15}+a_8A_{14}+a_8A_{11}A_{13}+A_6A_{13}+a_5a_{11}A_9\delta_1+a_5a_{11}a_{17}A_{12}+a_5a_{17}A_7\delta_1+a_5a_8A_{10}A_{13}+a_5a_8a_{18}A_{14}+a_5a_{18}A_6A_{13},$$

$$A_{26}=a_4a_9A_8\delta_1+a_4a_9A_0A_{12}+a_4a_{11}A_{11}A_{12}+a_4A_7A_{12}+a_4A_7A_{11}\delta_1+a_8A_8A_{15}+A_0A_6A_{15}+a_8A_{11}A_{14}+A_6A_{14}+A_6A_{11}A_{13}+a_5a_{11}A_9A_{12}+a_5A_7A_9\delta_1+a_5a_{17}A_7A_{12}+a_5a_8A_{10}A_{14}+a_5A_6A_{10}A_{13}+a_5a_{18}A_6A_{14},$$

$$A_{27}=a_4a_9A_8A_{12}-a_4A_7A_{11}A_{12}+A_6A_8A_{15}+A_6A_{11}A_{14}+a_5A_7A_9A_{12}+a_5A_6A_{10}A_{14},$$

$$A_{28}=a_5a_8A_0\delta_1+a_5a_8a_{16}A_{12}+a_5a_{16}A_6\delta_1,$$

$$A_{29}=a_5a_8A_8\delta_1+a_5a_8A_0A_{12}+a_5A_0A_0\delta_1+a_5a_{16}A_6A_{12},$$

$$A_{30}=a_5a_8A_8A_{12}+a_5A_6A_8\delta_1+a_5A_0A_6A_{12},\ A_{31}=a_5a_8a_{16}\delta_1,$$

$$A_{32}=A_{28}-A_{24},\ A_{33}=A_{29}+A_{21}-A_{25},\ A_{34}=A_{30}+A_{22}-A_{26},$$

$$A_{35}=a_5A_6A_8A_{12}+A_{23}-A_{27},\ A_{36}=a_3a_7-a_6A_3-a_2A_4+a_6A_2^2,$$

$$A_{37}=a_3A_5+A_2^2A_4+A_3A_4,$$

$$A_{38}=a_8a_{18}A_{15}+a_8A_{12}+a_8A_{11}\delta_1+A_6\delta_1-a_9a_{17}\delta_1,$$

$$A_{39}=a_8A_{10}A_{15}+a_{18}A_6A_{15}+a_8A_{11}A_{12}+A_6A_{12}+A_6A_{11}\delta_1+a_{17}a_{29}A_{15}-a_{13}a_{29}\delta_1-a_9a_{17}A_{12}-a_9A_9\delta_1-a_9a_{13}a_{18}\delta_1,$$

$$A_{40}=A_6A_{10}A_{15}+A_6A_{11}A_{12}+a_{29}A_9A_{15}-a_{13}a_{29}A_{11}\delta_2-a_9A_9A_{12}-a_9a_{13}A_{10}\delta_2,$$

$$A_{41}=a_2a_6A_{38}-a_8\delta_1A_{36},\ A_{42}=a_2a_6A_{39}+A_{36}A_{38}-a_8\delta_1A_{37},$$

$$A_{43}=a_2a_6A_{40}-A_{37}A_{38}-A_{36}A_{39},\ A_{44}=A_{37}A_{39}+A_{36}A_{40},$$

$A_{45}=a_2a_6A_{32}+A_{16}A_{31}+a_2a_6a_8\delta_1,\ A_{46}=a_2a_6A_{33}+A_{16}A_{32}+A_{17}A_{31}+A_{41},$

$A_{47}=a_2a_6A_{34}+A_{16}A_{33}+A_{17}A_{32}+A_{42},\ A_{48}=a_2a_6A_{35}+A_{16}A_{34}+A_{17}A_{33}+A_{43},$

$A_{49}=A_{16}A_{35}+A_{17}A_{34}-A_{44},\ A_{50}=A_{17}A_{35}-A_{37}A_{40},$

$$N_1=\frac{d_{31}}{a_2a_6A_{31}},\ N_2=\frac{d_{32}}{a_2a_6A_{31}},\ N_3=\frac{d_{33}}{a_2a_6A_{31}},\ N_4=\frac{d_{34}}{a_2a_6A_{31}},$$

$$N_5=\frac{d_{35}}{a_2a_6A_{31}},\ N_6=\frac{d_{36}}{a_2a_6A_{31}},\ A=\frac{A_{45}}{a_2a_6A_{31}},\ B=\frac{A_{46}}{a_2a_6A_{31}},$$

$$E=\frac{A_{47}}{a_2a_6A_{31}},\ F=\frac{A_{48}}{a_2a_6A_{31}},\ G=\frac{A_{49}}{a_2a_6A_{31}},\ H=\frac{A_{50}}{a_2a_6A_{31}}.$$

Appendix C

$$L_1=\frac{1}{(\gamma^{*12}-A\gamma^{*10}+B\gamma^{*8}-E\gamma^{*6}+F\gamma^{*4}-G\gamma^{*2}+H)},$$

$d_1=a_{20}\gamma^{*2}-A_1,\ d_2=a_2\gamma^{*2}-A_3,\ d_3=a_6\gamma^{*2}-A_4,\ d_4=a_7\gamma^{*2}-A_5,$

$d_5=a_8\gamma^{*2}-A_6,\ d_6=a_{11}\gamma^{*2}-A_7,\ d_7=a_{16}\gamma^{*4}-A_0\gamma^{*2}+A_8,$

$d_8=a_{17}\gamma^{*2}-A_9,\ d_9=a_{18}\gamma^{*2}-A_{10},\ d_{10}=\gamma^{*2}-A_{11},\ \mathrm{d}_{11}=\delta_1\gamma^{*2}-A_{12},$

$d_{12}=a_{13}\gamma^{*2}-A_{14},\ d_{13}=d_5d_{11}+a_{13}a_{29}\delta_2,\ d_{14}=a_9d_{11}+a_{29}A_{15},$

$d_{15}=d_6d_{11}-a_{29}d_{12},\ d_{16}=d_8d_{11}+a_{13}\delta_2d_9,\ d_{17}=d_{10}d_{11}-A_{15}d_9,$

$d_{18}=d_7d_{11}+d_9d_{12},$

$d_{19}=a_4d_2d_3d_{11}+a_3a_4d_4d_{11}-a_{13}\delta_2d_2d_3-a_3a_{13}\delta_2d_4,$

$d_{20}=a_5d_2d_3d_{11}+a_3a_5d_4d_{11}+A_{15}d_2d_3+a_3A_{15}d_4,$

$d_{21}=d_1d_2d_3d_{11}+a_3d_1d_4d_{11}+d_3d_{11}A_2^2-d_2d_3d_{12}-a_3d_4d_{12},$

$d_{22}=A_{15}d_5-a_9a_{13}\delta_2,\ d_{23}=a_9d_{11}+a_{29}A_{15},\ d_{24}=A_{15}d_6+a_9d_{12},$

$d_{25}=A_{15}d_8+a_{13}\delta_2d_{10},\ d_{26}=d_{10}d_{11}-A_{15}d_9,\ d_{27}=d_{10}d_{12}+A_{15}d_7,$

$d_{28}=a_4A_{15}d_2d_3+a_4A_{15}d_4+a_5a_{13}\delta_2d_2d_3+a_5a_{13}\delta_2d_4,$

$d_{29}=A_{15}d_2d_3+A_{15}d_4+a_5d_2d_3d_{11}+a_5d_4d_{11};$

$d_{30}=A_{15}d_1d_2d_3+A_{15}d_1d_4+A_{15}A_2^2d_3+a_5d_2d_3d_{12}+a_5d_4d_{12},$

$d_{31}=a_{29}d_{16}^2d_{21}+d_9d_{13}d_{16}d_{21}-a_{29}d_{16}d_{18}d_{19}+d_2d_3d_{13}d_{16}d_{18}+a_3d_4d_{13}d_{16}d_{18}$

$d_{32}=a_{29}d_{16}^2d_{20}+d_9d_{13}d_{16}d_{20}-a_{29}d_{16}d_{17}d_{19}+d_2d_3d_{13}d_{16}d_{17}+a_3d_4d_{13}d_{16}d_{17}$

$\quad -d_9d_{14}d_{16}d_{19}-d_2d_3d_{14}d_{16}^2-a_3d_4d_{14}d_{16}^2,$

$d_{33}=a_{29}d_{17}d_{18}d_{21}-a_{29}d_{18}^2d_{20}-d_9d_{15}d_{18}d_{20}+d_9d_{14}d_{18}d_{21}+d_2d_3d_{14}d_{18}^2$

$\quad +a_3d_4d_{14}d_{18}^2-d_2d_3d_{15}d_{17}d_{18}-a_3d_4d_{15}d_{17}d_{18},$

$d_{34}=a_9d_{18}d_{27}d_{28}+a_5d_2d_3d_{22}d_{27}^2+a_3a_5d_4d_{22}d_{27}^2-d_{10}d_{22}d_{27}d_{30}$

$\quad +a_5d_2d_3d_{24}d_{25}d_{27}+a_3a_5d_4d_{24}d_{25}d_{27}-a_9d_{18}d_{25}d_{30}-d_{10}d_{24}d_{27}d_{28},$

$d_{35}=-A_2d_3d_{32},$

$d_{36}=A_2d_3d_4(a_{29}d_{16}^2d_{21}+d_9d_{13}d_{16}d_{21}-a_{29}d_{16}d_{18}d_{19}+d_2d_3d_{13}d_{16}d_{18}$

$\quad +a_3d_4d_{16}d_{18}-d_9d_{15}d_{16}d_{19}-d_2d_3d_{15}d_{16}^2-a_3d_4d_{15}d_{16}^2),$

$d_{37}=N_2L_1\{\gamma^{*2}-[\frac{2}{r^2}+(\frac{2x}{r^2}+iR)^2]\},\ d_{38}=L_1[N_2(-\frac{2x}{r^2}-iR)-N_5\gamma^*],$

$d_{39}=L_1[-N_2\gamma^*-N_5(-\frac{2x}{r^2}-iR)],$

$d_{41}=a_{30}d_{27}+a_{22}\mathrm{N}_3L_1-\mathrm{N}_4L_1-a_5\mathrm{N}_1L_1,$

$d_{40}=a_{30}d_{37}+a_{22}N_3L_1-N_4L_1-a_5N_1L_1+a_{23}d_{38}(-\frac{2x}{r^2}-iR)-\frac{2L_1N_1}{r^2},$

$d_{42}=d_{41}-a_{23}d_{39}\gamma^*,$

$d_{43}=a_{24}[d_{39}(-\frac{2x}{r^2}-iR)-d_{38}\gamma^*-\frac{2L_1N_5}{r^2}]+a_3[d_{39}(-\frac{2x}{r^2}-iR)$

$\quad +N_6L_1-\frac{2L_1N_5}{r^2}],$

$d_{44}=a_{24}[d_{39}(-\frac{2x}{r^2}-iR)-d_{38}\gamma^*-\frac{2L_1N_5}{r^2}]-a_3(N_6L_1+d_{38}\gamma^*),$

$d_{45}=a_{25}N_6L_1(-\frac{2x}{r^2}-iR)+\gamma^*a_{26}N_3L_1,$

$d_{46}=-a_{25}N_6L_1\gamma^*+a_{26}N_3L_1(-\frac{2x}{r^2}-iR),$

$d_{47}=a_{28}N_3L_1(-\frac{2x}{r^2}-iR)-a_{26}N_6L_1\gamma^*,$

$d_{48}=-a_{28}\gamma^*N_3L_1-a_{26}N_6L_1(-\frac{2x}{r^2}-iR),$

$$H_{1n}=\frac{-A_2(a_6k_n^2-A_4)}{[(a_6k_n^2-A_4)(a_2k_n^2-A_3)+a_3a_7k_n^2-a_3A_5]},$$

$$H_{2n}=\frac{-H_{11}(a_7k_n^2-A_5)}{(a_6k_n^2-A_4)},$$

$$H_{3n}=\frac{-[s_{10}k_n^4-s_{11}k_n^2+s_{12}+H_{1n}(s_{13}k_n^2+s_{14})]}{(a_8s_2k_n^4+s_{15}k_n^2-s_{16})},$$

$$H_{4n}=\frac{-[s_8k_n^2-a_{29}A_2H_{1n}+H_{3n}(a_8k_n^2-s_7)-s_9]}{s_1},$$

$H_{5n}=a_{20}k_n^2-A_1-A_2H_{1n}+a_4H_{3n}-a_5H_{4n},\ H_{6n}=k_n^2-R^2,$

$H_{7\mathrm{n}}=\mathrm{i}R-k_nH_{2\mathrm{n}},\ H_{8\mathrm{n}}=-(k_n+\mathrm{i}RH_{2n}),$

$H_{9\mathrm{n}}=a_{30}H_{6\mathrm{n}}+a_{22}H_{3\mathrm{n}}-H_{4\mathrm{n}}-a_5H_{5\mathrm{n}}+ia_{23}RH_{7\mathrm{n}},$

$H_{10\mathrm{n}}=a_{30}H_{6\mathrm{n}}+a_{22}H_{3\mathrm{n}}-H_{4\mathrm{n}}-a_5H_{5\mathrm{n}},\ H_{11\mathrm{n}}=H_{10\mathrm{n}}-\mathrm{a}_{23}k_n,$

$H_{12\mathrm{n}}=-a_{24}H_{7\mathrm{n}}k_n+\mathrm{i}a_{24}RH_{8\mathrm{n}}+\mathrm{i}a_3RH_{8\mathrm{n}}+a_3H_{1\mathrm{n}},$

$H_{13\mathrm{n}}=-a_{24}H_{7\mathrm{n}}k_n+\mathrm{i}a_{24}RH_{8\mathrm{n}}-a_3k_nH_{7\mathrm{n}}-a_3H_{1\mathrm{n}},$

$H_{14\mathrm{n}}=\mathrm{i}a_{25}RH_{1\mathrm{n}}+a_{26}k_nH_{3\mathrm{n}},$

$H_{15\mathrm{n}}=-a_{25}k_nH_{1\mathrm{n}}+\mathrm{i}a_{26}RH_{3\mathrm{n}},$

$H_{16\mathrm{n}}=\mathrm{i}a_{28}RH_{3\mathrm{n}}-a_{26}k_nH_{1\mathrm{n}},$

$H_{17\mathrm{n}}=-a_{28}k_nH_{3\mathrm{n}}-\mathrm{i}a_{26}RH_{1\mathrm{n}}.$